Journal of Electronic Testing (2022) 38:493–510
https://doi.org/10.1007/s10836-022-06022-x

Influence of Printed Circuit Board Dynamics on the Fretting Wear of Electronic Connectors: A Dynamic Analysis Approach

Sushil Doranga[1] · Jenny Zhou[1] · Ram Poudel[2]

Received: 22 April 2022 / Accepted: 23 August 2022 / Published online: 10 September 2022

Abstract
The harsh operating environment of automotive and aerospace applications causes printed circuit board (PCB) connectors to be susceptible to intermittent high contact resistance, which eventually leads to a failure resulting in the loss of signal integrity. Pin fretting within the mating connector is often the cause of these failures. Over the past several years, there has been a significant increase in the laboratory-based testing of sample connectors for pin fretting. These laboratory-based results have shown the primary cause of pin fretting to be due to the relative motion within the mating connector. However, quantification of the relative motion in different vibration environments by considering the dynamics of PCBs has not been studied yet. This paper develops a new methodology for studying pin fretting within the mating connector. The developed methodology is based on the quantification of relative motion as a measure of pin fretting by considering the dynamics of PCBs, printed circuit board assemblies (PCBAs), and mounting brackets. To do this, a continuous, lightly damped, multi-degree of freedom (MDOF) model is developed for the assembly consisting of PCBs, PCBAs, and mounting brackets. The behavior of the system is investigated by exciting the system using harmonic and random vibration signals. In the harmonic signal analysis, a frequency domain-based approach is presented to compute the relative motion of the mating connector, while a pseudo-random time series signal derived from the power spectrum density (PSD) of the signal is used to excite the system for the random vibration excitation analysis. The relative response vector is then computed based on the system's response. The results of the relative motion of the mating connectors are presented in terms of the maximum amplitude of relative motion and the cumulative relative movement. The significance of the cumulative relative movement is that the complex phenomenon of pin fretting in the mating connectors can be represented by a simple time series model that can be used to correlate the material degradation. Finally, two numerical examples using the analytical and finite element-based (FE) technique are shown to demonstrate the proposed methodology. The examples show that the method proposed here is systematic and constructive in quantifying the pin fretting behavior.

Keywords Model Formulation · Base Excitation · Relative Motion · Signal Analysis

1 Introduction

Electronic connectors are frequently used in printed circuit boards (PCBs) and are typically used to transfer signals or power from one PCB to another. Blade/receptable, eye of the needle, and other press fit connectors such as backplane connectors are widely used in the assembly of PCBs. Due to extreme vibration environments, fretting wear is one of the most common causes of premature connector failures. Fretting-induced wear results in a loss of normal contact force and eventually increases the electrical contact resistance in the contact pair.

The cause of fretting-induced wear in the connectors has gained considerable research interest over the years. An extensive overview of pin fretting in connectors is presented in reference [2], which presents detailed information on the mechanism that controls the onset and progression of fretting behavior. The experimental evaluations, their importance, and current status of the study of fretting

Responsible Editor: V. D. Agrawal

✉ Sushil Doranga
sdoranga@lamar.edu

[1] Department of Mechanical Engineering, Lamar University, Beaumont, TX 77710, USA

[2] Department of Sustainable Technology and the Built Environment, Appalachian State, University, Boone, NC 28608, USA

degradation have been well documented in references [4, 5, 8, 18, 20].

Xie [18] examined vibration-induced fretting corrosion on single-row, pin-and-socket PC-type, and automotive-type connectors, taking into account the influence of the design of the connectors, length of the clamps, vibration profiles, and lubrication. Both connector designs were found to have consistent relative displacement limits for the onset of friction corrosion, regardless of the excitation frequency. Furthermore, fretting rates were found to be linearly dependent on input acceleration (g) for single-frequency harmonic excitation. Flowers et al. [4, 5] performed the sinusoidal step (harmonic excitation) test on a single-row tin-plated socket connector to determine the vibration threshold for fretting corrosion. During their experiments, the magnitude of input excitement varied across a range of g-levels. Their study concluded that the dynamic response of the mechanical system under various g-levels and tie-off configurations will greatly affect the contact wear rate of a connector system.

The friction degradation of the contacts in a coupling connector not only increases the electrical resistance but also produces a capacitance effect at the interface due to corrosion buildup. Yang et al. [20] conducted an experimental study to investigate the capacitance built up in a commercial connector pin as a result of fretting-induced vibration. A simpler model was developed to relate the capacitance behavior to connector characteristics, vibration profile, and resistance behavior. Their results showed the capacitive properties to be attributed due to a thicker layer of metal oxide building up with more vibration-induced fretting cycles.

Hsu and Liao [7] developed a finite element model to theoretically investigate fretting wear in a rectangular electrical connector consisting of the twist-pin/socket contact pair during insertion as well as harmonic vibration. Their investigation concluded that the damage caused by contact wear is due to the reduced contact area and increased contact resistance.

At present, most evaluations of fretting in connectors have focused on particular connector designs and the influence variations in these designs have on fretting performance and have been conducted through exhaustive experimental testing, which requires a major commitment of time and resources. Most of the studies described in the existing literature measure the normal forces in the mating connector, monitor electrical resistance, evaluate material degradation due to relative motion, and find the vibration thresholds for pin fretting [5–8, 11, 12, 15, 19]. However, no study is yet known to have analyzed connectors at the system level with respect to real-life applications.

While simulation-based methods well aligned with the experimental results are proposed in the literature, such methods are based solely on the connector level analysis [17, 22]. In PCB connectors, the degradation of pin quality within the mating connector depends on the coupled dynamics of the PCBs, mounting brackets, and heatsinks. This research seeks to develop: (i) a mathematical model that can be applied to the experimental system as well as a detailed finite element model that covers the dynamics of the PCB, heatsinks, and mounting brackets, which in turn will relate to the observed relative motion at the connector housing interface; (ii) an algorithm for detecting relative motion in the presence of harmonic and random vibration signals; and (iii) a mathematical model that relates the cumulative movement of the connectors to the materials' degradation. This method aims to shed light on variables such as input time history, power spectrum density, base excitation, and pseudo-random time series. The approach developed here is believed to be able to quantify relative motion within the mating connectors and to be usable by practicing engineers in the electronic industry for modifying designs to reduce pin fretting, as well as by scientists and researchers for solving pin fretting problems by developing suitable active and passive control systems.

The rest of the paper is organized as follows. Section 2 presents the overall methodology for computing the relative motion of mating connectors by considering the dynamics of PCBs, PCBAs, and mounting brackets. Section 3 presents a numerical example to demonstrate the proposed methodology. Section 4 presents the FE modeling procedure in the assembly of a backplane connector consisting of a PCB, heatsinks, card guides, and mounting brackets, as well as the results from the FE model. Section 5 concludes the paper with the results of the research and the significance of the presented work.

2 Methodology for the Quantification of Pin Fretting

This section presents a brief theory for quantifying pin fretting as a measure of relative motion within the mating connector. The presented theory is based on the dynamics of an assembly consisting of a PCB, PCBAs, connectors, heatsinks, and mounting brackets using the base excitation as an input. Since most electronic components and assemblies are tested using an electrodynamic shaker, analyzing the dynamics of the system/assembly as a base-excited structure is crucial. Due to PCB connectors being used mostly in the transportation industries, including locomotive, automotive, and aerospace industries, the main source of vibrations are the harmonic (sinusoidal) vibrations coming from the engine and the random vibration (non-periodic motion) coming from the ground motion of a vehicle. Similarly, in the aerospace industry, the source of harmonic vibration is the engine itself, with the random vibration being the vibrations coming from aerodynamic action. Thus, analyzing both types of vibration signals

is crucial. For a harmonic signal analysis, a dynamic model is formulated as a hybrid modal space where the response vector is kept in the physical domain and all the remaining parameters in the modal domain. Since the responses of the mating connector yield the relative motion, pin fretting can be directly quantified based on the modal parameters, which is the benefit of using the hybrid modal space formulation. For a random vibration excitation, the input is usually presented in a condensed form known as power spectrum density (PSD). The PSD input to the model yields a response in the form of a PSD that has little to no meaning in the context of the relative motion. As such, a correlation function in the form of pseudo-random time series is developed, and the relative motion and the total cumulative movement of the mating connector are evaluated based on the pseudo-random time series excitation. The total cumulative movement of the connector will yield the material degradation per second within the connector as a result of pin fretting.

2.1 Mathematical Formulation for the Relative Motion with Harmonic Input

Consider a MDOF system representing an assembly composed of PCBs, PCBAs, heatsinks, and mounting brackets subjected to base excitation. The general equation of motion can be represented as:

$$[M]\{\ddot{u}\} + [K]\{u\} + [C]\{\dot{u}\} = -[M]\{l\}\ddot{y} \tag{1}$$

where [M], [K], and [C] are the mass, stiffness, and proportional damping matrices of the system in a fixed base configuration, $\ddot{y}$ is the input acceleration, $\{u\}$ is the vector of displacement relative to the base, and $\{l\}$ is the transformation vector ($\{l\}_i = Cos(\theta)_i$) with $(\theta)_i$ is the angle between the i^{th} degree of freedom and the direction of base motion. Transforming Eq. (1) to the frequency domain allows it to be rewritten as:

$$\left[-\omega^2[M] + [K] + i\omega[C]\right]\{U\} = \omega^2[M]\{l\}Y \tag{2}$$

For a lightly damped system, the modal matrix $[\Phi]$ can be obtained by solving the undamped free vibration equation of motion obtained from the left side of Eq. (1), and the model can be defined in the hybrid form using the modal matrix, where the response vectors are in the physical coordinate system, and all the remaining parameters are in the modal domain.

Multiplying both sides of Eq. (2) by the modal matrix $[\Phi]^T$ and introducing the term $[\Phi][\Phi]^{-1} = [I]$, Eq. (2) then becomes:

$$\begin{aligned}\left[-\omega^2[M] + [K] + i\omega[C]\right][\Phi]^T[\Phi][\Phi]^{-1}\{U\} \\ = \omega^2[\Phi]^T[\Phi][\Phi]^{-1}[M]\{l\}Y\end{aligned} \tag{3}$$

For the mass normalized mode shapes matrix and proportional damping assumptions, the orthogonal properties of the linear modal matrix $[\Phi]$ can be written as:

$$[\Phi]^T[M][\Phi] = [I] \tag{4}$$

$$[\Phi]^T[K][\Phi] = \left[\omega_r^2\right]_{diag} \tag{5}$$

$$[\Phi]^T[C][\Phi] = \left[2\zeta_r\omega_r\right]_{diag} \tag{6}$$

Substituting Eqs. (4), (5), and (6) into Eq. (3) allows Eq. (3) to be rewritten as:

$$\left[-\omega^2[I] + \left[\omega_r^2\right]_{diag} + i\omega\left[2\zeta_r\omega_r\right]_{diag}\right][\Phi]^{-1}\{U\} = \omega^2[\mathrm{I}][\Phi]^{-1}\{l\}Y \tag{7}$$

Let $\left[\left[\omega_r^2\right]_{diag} + i\omega\left[2\zeta_r\omega_r\right]_{diag} - \omega^2[I]\right] = \left[\lambda - \omega_r^2\right]$

where the bracket $\left[\lambda - \omega_r^2\right]$ denotes a diagonal matrix. Using this property, Eq. (7) can be rewritten more concisely as:

$$\left[\lambda - \omega_r^2\right][\Phi]^{-1}\{U\} = \omega^2[\Phi]^{-1}\{l\}Y \tag{8}$$

Here, $-\omega^2 Y = A$ is the base acceleration in the frequency domain.

$$\{U\} = [\Phi]\left[\lambda - \omega_r^2\right]^{-1}[\Phi]^{-1}\{l\}A \tag{9}$$

Equation (9) represents the hybrid model for the MDOF system undergoing base excitation. The response vector $\{U\}$ shown in Eq. (9) can be extracted from the FE-based model, as well as from the experimental data if the system's modal parameters are known. Computing the response vector $\{U\}$ from the male and female connectors will yield the relative motion within the mating connector.

2.2 Computation of Relative Motion with Random Vibration Input

The random vibration profiles for testing electronic components are usually presented in the form of PSD. Implementing the PSD profile in the experimental setup using the electrodynamic shaker and measuring the response vector in the form of a time series has been a straightforward approach. However, applying the PSD-based profile to the theoretical model poses a challenge for computing relative motion. The PSD input to the theoretical model will result in the output being in PSD form. The response in PSD form will have little to no meaning in the context of relative motion. Therefore, an approach has been developed to generate the pseudo-random time series (correlation function) from the PSD signal. The correlation function (pseudo-random time

series) has a root mean square amplitude equivalent to the original PSD, with the frequency component paired to the original PSD. The pseudo-random time series can then be implemented in a modal domain to obtain the relative motion of the connectors. To develop a pseudo-random time series from the user's PSD function, the following steps are used:

2.2.1 Generating the White Noise Time History

A white noise acceleration time series is generated using the random number function in MATLAB. The white noise is generated with a mean of zero and finite variance and is expected to repeat over a certain interval of time. The sample time is chosen in such a way that it covers at least the input frequency range of the user's PSD function.

2.2.2 Fourier Spectrum of White Noise Time History

The time series white noise signal is taken over to the frequency domain using the Fourier transformation method. The amplitude spectrum thus obtained is then scaled by the arbitrary factor to meet the user's PSD function. The root mean square (rms) value of the time series signal is compared to the rms value of the PSD function. The scaling process continues until the rms value of the time series matches the user's PSD.

2.2.3 Computation of Relative Motion using Pseudo Random Time Series

Consider the MDOF system subjected to the base excitation defined in Sect. 2.2. Recalling Eq. (1) and using $\{u\} = [\Phi]\{q\}$ where $\{q\}$ is the modal coordinate, Eq. (1) can be rewritten in the modal space as:

$$[M][\Phi]\{\ddot{q}\} + [K][\Phi]\{q\} + [C][\Phi]\{\dot{q}\} = -[M]\{l\}\ddot{y} \tag{10}$$

Multiplying both sides by transposing the mass-normalized orthogonal mode shape's matrix $[\Phi]^T$, Eq. (10) can be rewritten as:

$$[\Phi]^T[M][\Phi]\{\ddot{q}\} + [\Phi]^T[K][\Phi]\{q\} + [\Phi]^T[C][\Phi]\{\dot{q}\} = -[\Phi]^T[M]\{l\}\ddot{y} \tag{11}$$

Using Eqs. (4), (5), and (6), Eq. (11) can be further rewritten as:

$$\{\ddot{q}\} + \left[\omega_r^2\right]_{diag}\{q\} + \left[2\zeta_r\omega_r\right]_{diag}\{\dot{q}\} = -[\Phi]^T[M]\{l\}\ddot{y} \tag{12}$$

Equation (12) can be solved in the time domain using the pseudo-random time series if the mass distribution of the structure is known a priori. This equation can be used in the experimental model as well as the FE-based model, and the relative response vector can be calculated once the modal displacements for each considered mode are obtained. The response vector can be obtained through the modal superposition. The relative motion within the mating connector can be calculated based on the response from the mating connectors.

The relative motion within the mating connector can be formulated as:

$$r(t) = u_m(t) - u_f(t) \tag{13}$$

where $u_m(t)$ is the time series response of the male connector, $u_f(t)$ is the time series response of the female connector, and $r(t)$ is the relative motion over the excitation time. The cumulative movement of the mating connector over the measured period can be formulated as:

$$M = \sum_{k=0}^{n-1} \left| \left(r\left(t_{k+1}\right) - r\left(t_k\right) \right) \right| \tag{14}$$

where n is the length of the time history, and $r\left(t_k\right)$ represents the relative motion at time t_k. The absolute value sign is used so as to include the positive and negative relative motions. Equation (14) represents the total cumulative movement over the excitation time period. This will be directly proportional to the degradation of pin coating materials within the mating connector. The measurement of relative motion directly in the pins is not feasible through experiments because the dimensions of the pin are very small. In reference [2], the relationship between the housing motion and the actual relative motion at the connector interface was evaluated using PC-type connector samples that were specially modified to allow direct measurements access to the terminal. The relative motion of the plug housing/header and the terminal header tended to be quite similar except for small differences at vibration frequencies near the respective resonance peaks. This shows that the contribution of the pin dynamics is negligible because of the pins' negligible mass.

3 Numerical Example to Demonstrate the Computation of Relative Motion

This section has preferred a 2 DOF lumped parameter model to demonstrate the methodology presented in Sect. 2. A model consisting of two masses that can be idealized as a female connector with a motherboard as one mass and the male connector with the daughter board as another mass subjected to base excitation is taken for analysis [14]. The 2 DOF model is shown in Fig. 1. Two rigid supports are used to constrain mass 1 and mass 2, and the uniform base excitation of acceleration $\ddot{y}_g$ is applied to the two rigid supports. The mass, damping, and stiffness parameters are assumed to yield simple mode shapes in order to simplify computation. If x_1 and x_2 are the absolute displacements of m_1 and m_2, and u_1 and u_2 are the relative displacement of m_1 and m_2 with respect to the rigid

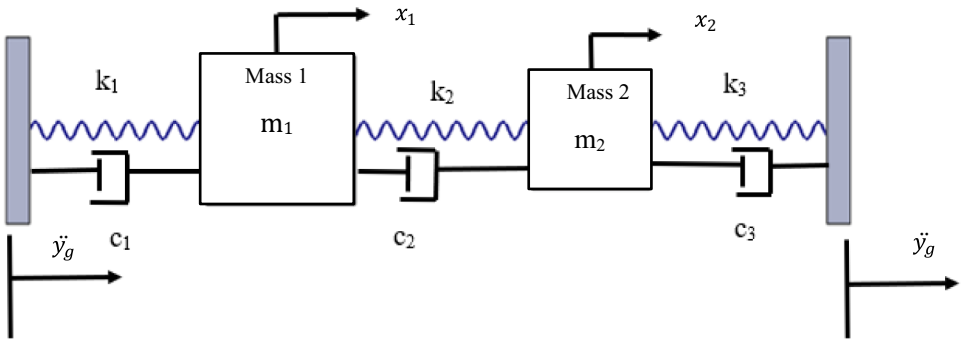

Fig. 1 The two DOF system subjected to base excitation

supports /moving base, then the equation of motion of the system in the matrix form can be written as:

$$\begin{bmatrix} m_1 & 0 \\ 0 & m_2 \end{bmatrix} \begin{Bmatrix} \ddot{u}_1 \\ \ddot{u}_2 \end{Bmatrix} + \begin{bmatrix} k_1 + k_2 & -k_2 \\ -k_2 & k_2 + k_3 \end{bmatrix} \begin{Bmatrix} u_1 \\ u_2 \end{Bmatrix} + \begin{bmatrix} c_1 + c_2 & -c_2 \\ -c_2 & c_2 + c_3 \end{bmatrix} \begin{Bmatrix} \dot{u}_1 \\ \dot{u}_2 \end{Bmatrix} = -\begin{bmatrix} m_1 & 0 \\ 0 & m_2 \end{bmatrix} \begin{Bmatrix} 1 \\ 1 \end{Bmatrix} \ddot{y}_g \tag{15}$$

where $\ddot{u}_1 = \ddot{x}_1 - \ddot{y}_g$, $\ddot{u}_2 = \ddot{x}_2 - \ddot{y}_g$, $\dot{u}_1 = \dot{x}_1 - \dot{y}_g$ and $u_1 = x_1 - y_g$. The parameters used for the simulation are $m_1 = 2$ kg, $m_2 = 1$ kg, $k_1 = k_3 = 5 \times 10^5$ N/m, $k_2 = 1 \times 10^5$ N/m, $c_1 = 202.86$Ns/m, $c_2 = 15.18$Ns/m, $c_3 = 139.37$Ns/m. The damping coefficients are chosen in such a way that the modal damping ratios for both modes are identical and equivalent to 10%.

3.1 Relative Motion Computation in the Harmonic Excitation

This section computes the relative motion between the two masses using the theoretical methodology developed in Sect. 2. As mentioned in Sect. 2, the methodology can be implemented in the FE-based model, thus the numerical results obtained using Eq. (9) can be compared to the FE-based model developed using the ANSYS 19.2 structural analysis tool.

The mode shapes and natural frequencies of the system shown in Fig. 1 are solved using the undamped equation of motion without excitation. The unexcited equation of motion for the undamped system shown in Fig. 1 can be written as:

$$\begin{bmatrix} m_1 & 0 \\ 0 & m_2 \end{bmatrix} \begin{Bmatrix} \ddot{u}_1 \\ \ddot{u}_2 \end{Bmatrix} + \begin{bmatrix} k_1 + k_2 & -k_2 \\ -k_2 & k_2 + k_3 \end{bmatrix} \begin{Bmatrix} u_1 \\ u_2 \end{Bmatrix} = 0 \tag{16}$$

The resulting natural frequencies and mode shapes of the undamped system are numerically computed and tabulated in Table 1. Once the mode shapes and the natural frequencies are obtained, the excitation frequency is varied over a frequency ranging from 5–180 Hz, keeping the amplitude at an excitation of 1 g (constant). For each excitation frequency, the steady state amplitude response of the system is solved using Eq. (9) and presented in the frequency domain.

The FE model of the 2 DOF freedom system shown in Fig. 1 is developed using the program ANSYS 19.2. Figure 2 shows the model developed in ANSYS using hexahedral 20-node solid elements. Spring connectors are used to connect mass 1, mass 2, and rigid supports. The undamped natural frequencies are obtained by performing the modal analysis with fixed rigid supports, with the two masses allowed to move only in longitudinally. Table 1 shows the natural frequencies that resulted from ANSYS. The natural frequencies computed from ANSYS are very close to the numerically computed values. The modal analysis results

Table 1 Natural Frequencies and Mode Shapes

Numerical Computation			ANSYS Computation
Modal Frequencies (Hz)	Mode Shapes		Modal Frequencies (Hz)
	1	2	
84.84	-0.6900	-0.1545	84.90
124.90	-0.2185	0.9758	125.20

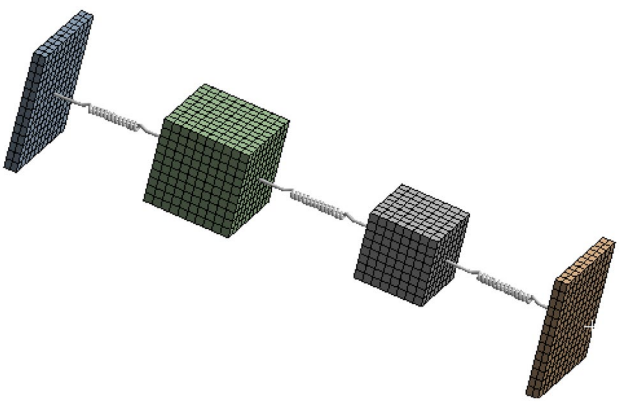

Fig. 2 2 DOF model in ANSYS

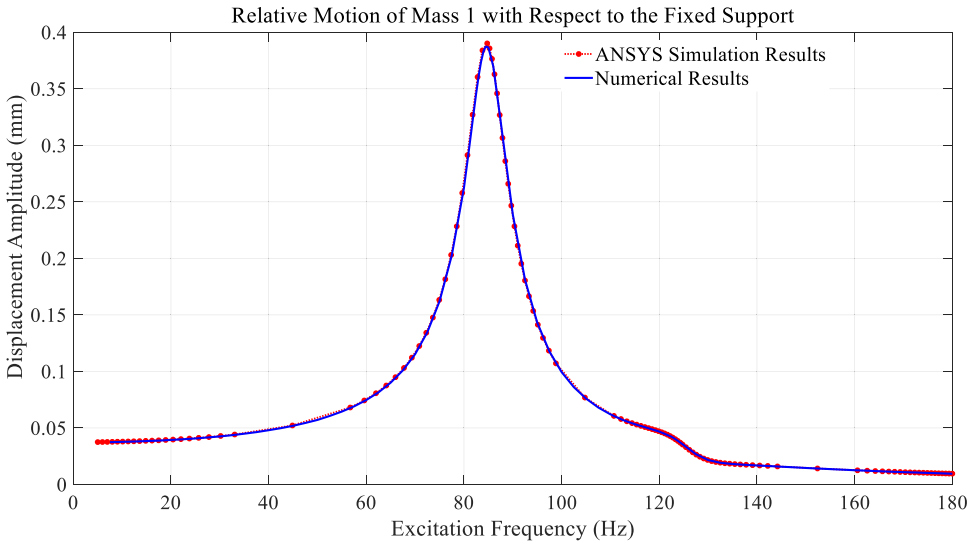

Fig. 3 Relative motion of mass 1 with respect to the fixed frame

thus obtained from the ANSYS modal tool are then connected to the ANSYS harmonic tool, and the harmonic analysis is carried out using a modal damping ratio of 0.1 for each mode. In order to use Eq. (9) in the ANSYS solver, the modal superposition method is applied to the ANSYS solution method, and a harmonic excitation of 1 g acceleration input is applied to the rigid support at a frequency range of 5–180 Hz.

The results obtained from the ANSYS solver are then compared with the numerically computed solution. Figures 3 and 4 show the comparison of the relative displacement results for mass 1 and mass 2 with respect to the rigid support. The results shown in Figs. 3 and 4 are the results representing the maximum amplitude of vibration at each excitation frequency. Figure 5 shows the relative motion between mass 1 and mass 2 as computed using Eq. (9) and the results obtained from ANSYS. In order to obtain the relative motion between masses 1 and 2, Eq. (9) is applied at each excitation frequency, and the response vectors are transformed to the time domain using the inverse fast Fourier transform (IFFT). The maximum relative motion at each excitation frequency is computed by calculating the absolute value of the difference in motion between masses 1 and 2. Similarly, the results from ANSYS are computed by calculating the maximum steady state amplitudes of the real and imaginary responses of the masses at each excitation frequency and then computing the absolute difference of the amplitude between mass 1 and mass 2. As shown in Fig. 5, the relative motion is maximum around the resonance frequency, which signifies that pin fretting due to vibration will be at its maximum when excitation occurs around the resonance frequency. The results obtained from the numerical computation using Eq. (9) and the ANSYS solver are very similar to each other in all three figures.

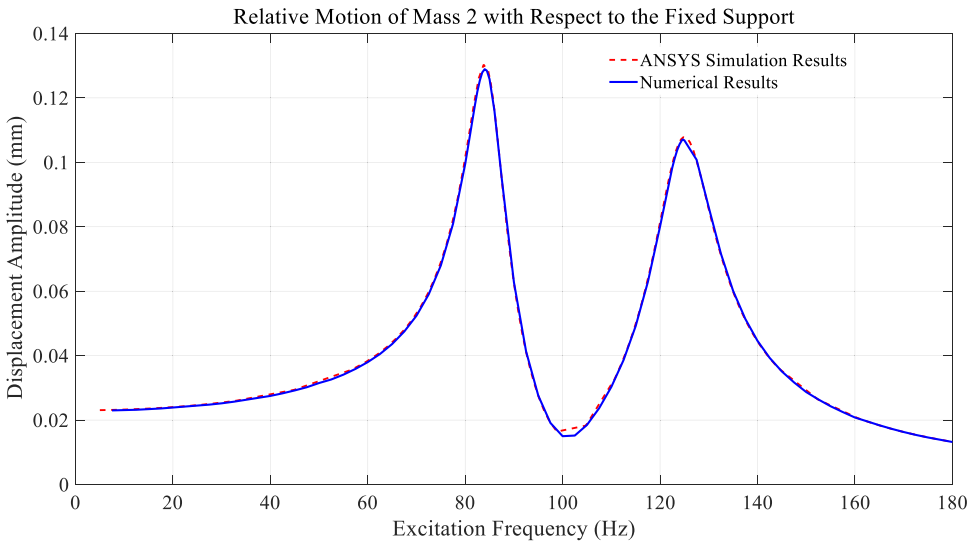

Fig. 4 Relative motion of mass 2 with respect to the fixed support

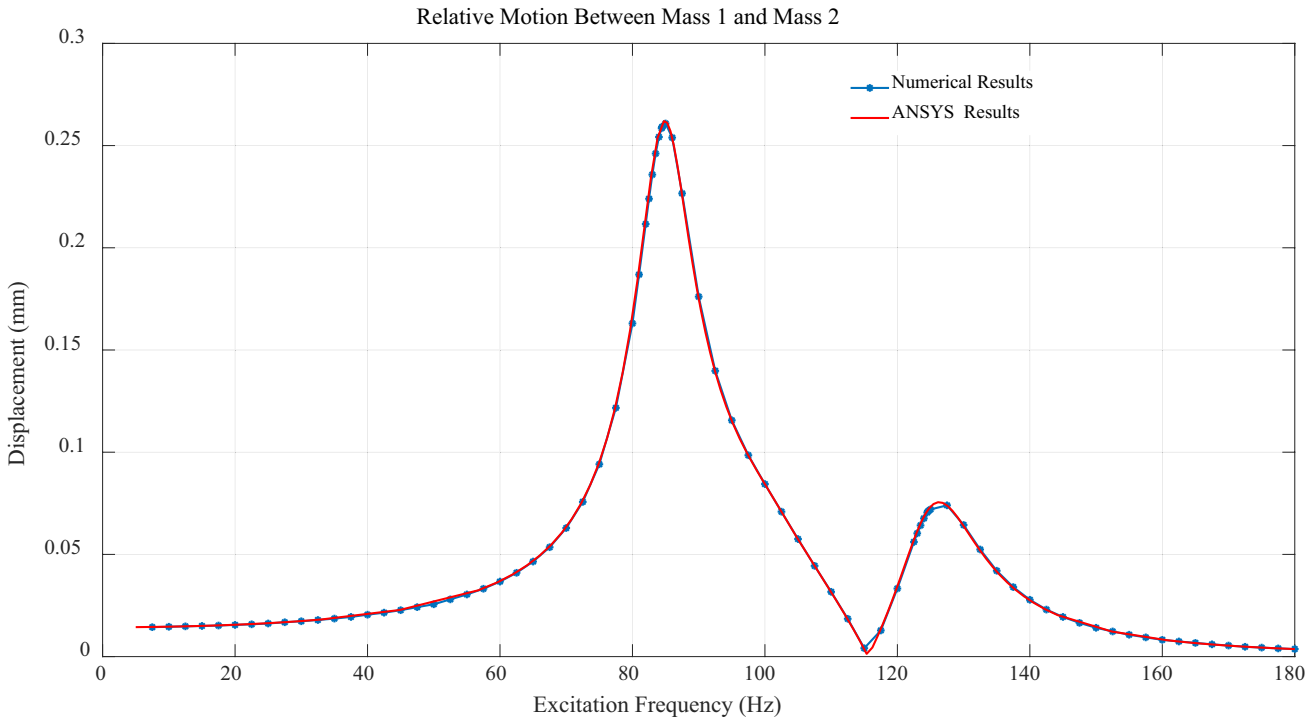

Fig. 5 Relative motion between mass 1 and mass 2

3.2 Relative Motion Computation using the White Noise Random Vibration Input

In this section, the model shown in Fig. 1 is analyzed for the random vibration input. The numerically simulated results using the random vibration as an input are compared with the simulation results obtained from ANSYS. In order to perform the comparison, the Gaussian white noise time series is generated using the *randn* function in MATLAB. The generated time series is used as an input excitation and the time domain responses of the model shown in Fig. 1 are computed by implementing the Runge–Kutta procedure in Eqs. (17) and (18). The model responses obtained in this way are then transformed into the physical coordinate system using the mode shapes matrix shown in Table 1. Similarly, the natural frequencies and undamped mode shapes obtained from the modal analysis tool in ANSYS are connected to the ANSYS transient analysis tool for the computation in ANSYS. A modal damping ratio of 0.1 is assigned for each mode, and the excitation in the form of white noise time series is applied as an excitation signal. The solution in ANSYS is computed using the iterative solver with fixed time steps.

By recalling Eqs. (10), (11), (12), and (15) and substituting the values for the mass, stiffness, damping coefficients, and the undamped mode shapes matrix, the equation of motion for the system shown in Fig. 1 can be written as:

$$\ddot{q}_1 + 16.9683\dot{q}_1 + 7.1981 \times 10^3 q_1 = 1.5985\ddot{y} \tag{17}$$

$$\ddot{q}_2 + 24.9805\dot{q}_2 + 1.5601 \times 10^4 q_2 = -0.6668\ddot{y} \tag{18}$$

where $\ddot{y}$ is the input excitation random time history. Equations (17) and (18) are solved for q_1 and q_2 using the Runge Kutta procedure. Once q_1 and q_2 are solved, the responses from mass 1 and mass 2 in the form of u_1 and u_2 are computed using the relation $\{u\} = [\Phi]\{q\}$, where $\{u\} = \begin{bmatrix} u_1 & u_2 \end{bmatrix}^T$. The numerically computed responses are then compared with the responses generated from the ANSYS transient analysis solver. The relative motion between mass 1 and mass 2 is computed using Eq. (13), and the total cumulative movement is calculated using Eq. (14). Figure 6 shows the comparison of the relative motion of mass 1 (u_1) with respect to the fixed base as generated using numerical computation and the ANSYS simulation. Figure 7 shows a close-up view of Fig. 6 and reveals some differences in amplitude of displacement between the numerically computed response and the ANSYS simulation. The difference is due to the computational error that occurred when solving ordinary differential equations. Similarly, Fig. 8 shows the response from mass 2 with respect to the fixed base. The overall idea of this paper is to generate the relative motion between mass 1 and mass 2 and find out the cumulative relative movement. The relative motion between masses 1 and 2 calculated using Eq. (13)

Fig. 6 Relative motion of mass 1 with respect to the fixed supports

is shown in Fig. 9. The total cumulative relative movement between masses 1 and 2 over 1 s is computed using Eq. (14), and the results are tabulated in Table 2. The total relative cumulative movements between masses 1 and 2 as computed using ANSYS and the numerical computation are very close to each other.

4 Computation of Relative Motion in Backplane PCB Connectors (Numerical Experiments)

The term backplane PCB generally refers to large format PCBs that are used as backbones for connecting several PCBs to ultimately form a computer bus. Typically, they do not contain active components but serve as a connection center between multiple PCBs. Examples include electronic units installed onboard for positive train control systems, event recorder systems, and communication and application management systems. The backplane PCB usually routes the signal from the main PCB to the other PCBs using a connector system known as a backplane connection system. Figure 10 shows the typical backplane connection system, where the main PCB is connected to the female connector and the backplane PCB is connected to the male connector. The connectors are assembled to the PCB using the press-fit technique. During vibration, a relative motion occurs within these mating pins' connector; as a result, a loss of the normal force will occur in the mating connector pins, which ultimately increases the resistance

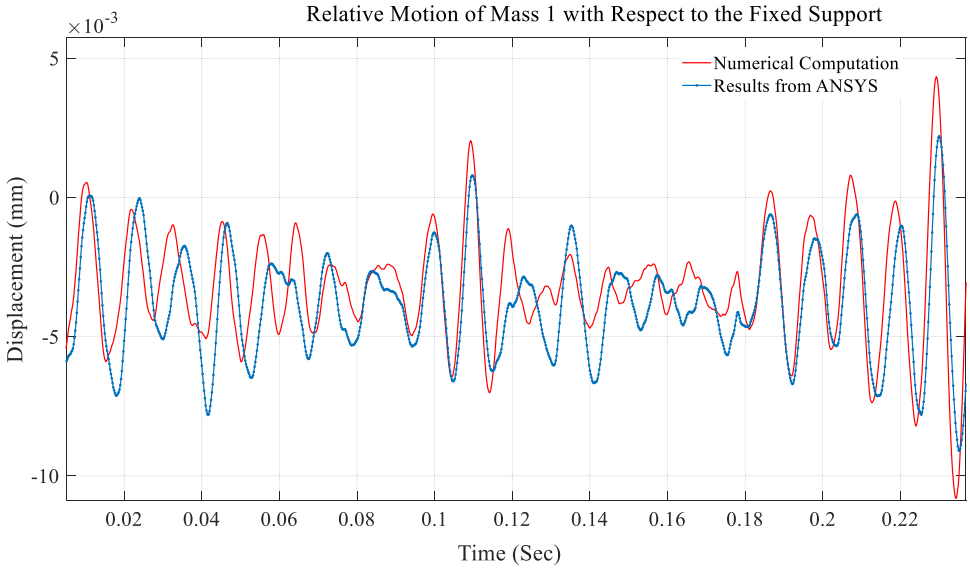

Fig. 7 Close-up view of Fig. 6

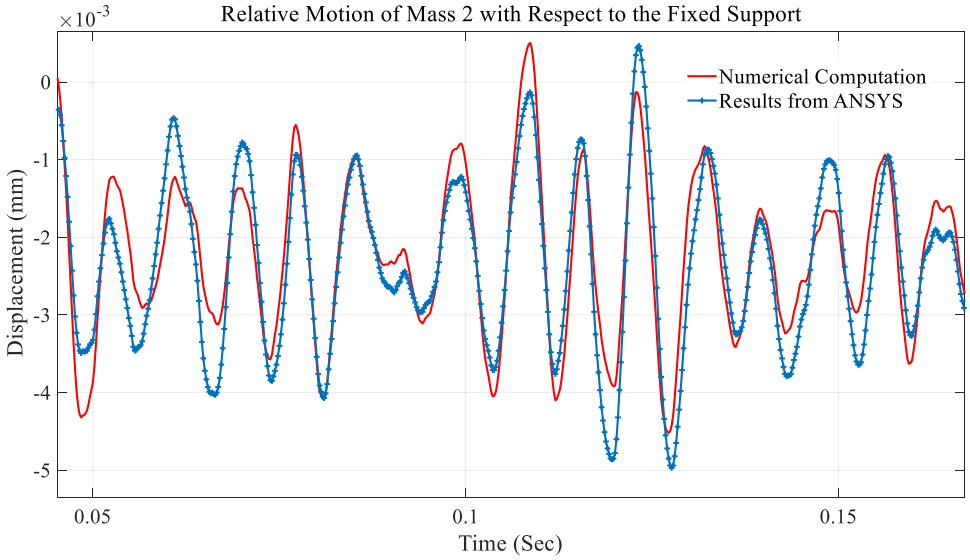

Fig. 8 Relative motion of mass 2 with respect to the fixed support

between the mating connector and results in the failure of the overall communication system. Yu et al. [22] studied the optimization of the contact resistance and insertion force of the backplane connector simultaneously by developing a mechanical model of a single contact pair. Their results yielded the optimum insertion force needing to be applied to mate a connector to induce minimum resistance in the contact. However, their study didn't account for the effect of vibrations on the mating connectors. The current paper, however, does deal with the vibration effect on the backplane connector using PCBs, heatsinks, and mounting brackets. Since the main board PCB contains several active components, heatsinks are used to solve thermal issues. Figure 11 shows an overall simplified model of a PC card-level assembly of PCBs to a backplane connector as used in practical cases. The main board PCB contains several active and passive components not modeled in this study. To prevent the damage caused by vibration and movement, PCB card guides are used [14]. The mating connector shown in Fig. 11 will transfer the signal from the main PCB to the backplane connector. The backplane will provide routing paths for several PCBs. Both the main PCB and backplane PCB will be connected to the chassis using a mechanical fastener not shown in this paper, as this paper deals only with a PCB card-level vibration analysis. Holes are also present in the mounting bracket for the bolts that are not shown in Fig. 11, as the feature of these bolts will be replicated through a beam connection in ANSYS.

Clearly what is of interest here is the development of an approach where the relative motion within a mating

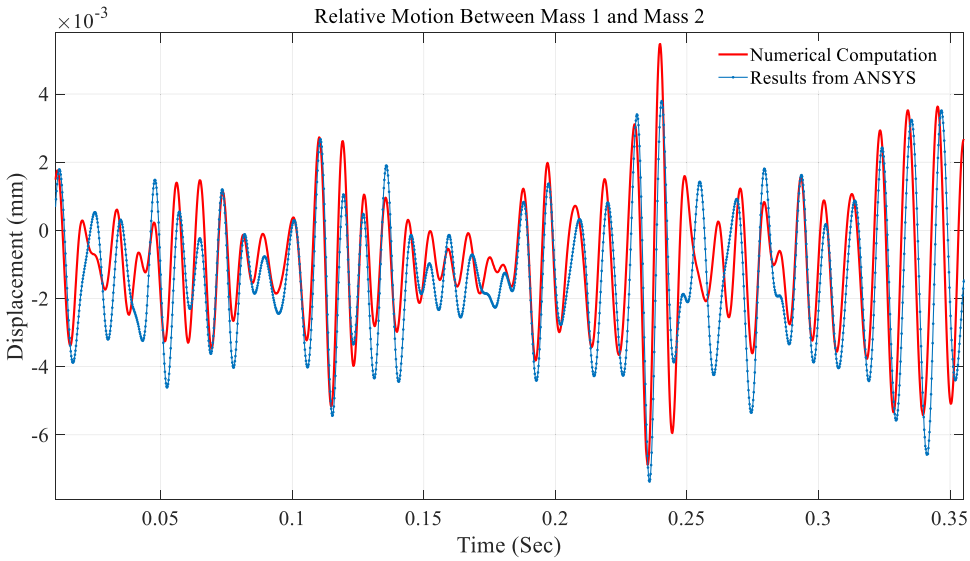

Fig. 9 Relative motion between mass 1 and mass 2

Table 2 Comparison of Relative Motion between Mass 1 and Mass 2 in 1 s Time Series

	Maximum Amplitude of Relative Motion (mm)	Total Cumulative Relative Movement per second (mm)
Results from ANSYS Solver	0.0127202	0.9001
Numerical Computation Results	0.01243	0.8709

connector can be quantified using the methodology developed in Sect. 2 when implemented using laboratory-based experiments as well as during in-service vibrations. To achieve this, a suitable fixturing procedure is developed such that the overall assembly can be tested in the base-excited shaker table (i.e., electrodynamic shaker table). Figure 12 shows one overall assembly that can be implemented in the base-excited shaker table. It consists of a fixture between the slip table and the PCB card assembly, an angle bracket to support the card guide, and L-brackets and a vertical plate to hold the PCB. All these components are designed in such a way that the natural frequencies of these fixture components are higher than the first mode natural frequency of the PCB card assembly shown in Fig. 11. The card-level assembly along with the fixtures shown in Fig. 12 are then implemented in the ANSYS structural analysis tool in order to apply the procedure developed in Sect. 2.

4.1 Developing the FE Model in ANSYS

The finite element model of the system shown in Fig. 12 is developed using the ANSYS structural analysis tools. The model development consists of: (i) cleaning up the geometry, (ii) applying the proper contact conditions, (iii) assigning the material properties to the individual components,

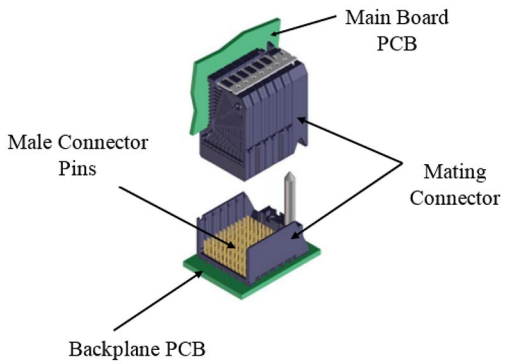

Fig. 10 A backplane connection system

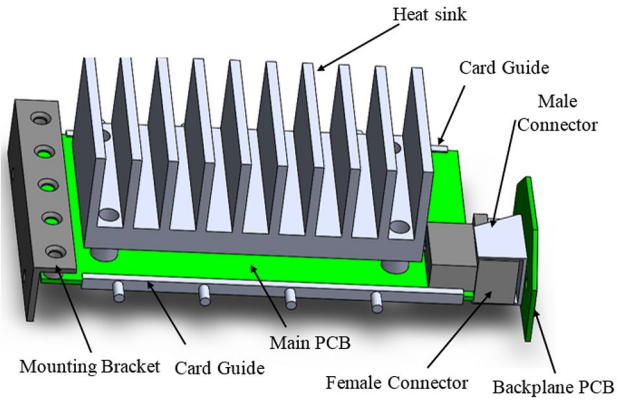

Fig. 11 A PCB with a backplane connector and mechanical components

(iv) developing the mesh model, and (v) applying the proper boundary condition. Cleaning up the geometrical model starts with removing the sliver faces and simplifying the geometry such that it contains no distorted elements. The actual geometrical model of the PCB and backplane connector shown in Fig. 11 are modified by removing the sharp edges and sliver faces. The modifications can be seen in Figs. 13 and 14. The pins in the connectors are removed, and the contact condition between the mating connector is modeled by applying the translational joint between the connector housing instead of applying the contact conditions in the connector pins that are double cantilevered. The translational joint will model the mating connector as the sliding contact motion. This is done under the assumption made for this analysis that the relative motion within the housing of the mating connector is equivalent to the relative motion between the mating pins. Some minor differences will occur in the relative motion in the housing and mating pins, as reported in references [2, 18], with the main difference being noted around the resonance frequency. However, from a practical aspect, all pins will not degrade equally, nor is measuring the response at the connector pins possible.

The housing for the connector in the PCB is a press-fit connection, and the press-fit contact model is developed through a bonded contact with the coefficient of friction between the contact surfaces being 0.1. Similarly, several screw connections occur between the PCB and heatsinks, the mounting brackets and PCBs, the card guide and card guide fixture, and the backplane PCB and backplane fixture, with beam bolts being used to address the screw connections [3]. The beam bolts are made using a body-to-body beam connection. The beam connection creates constraint equations between the beam nodes and the reference and mobile surfaces. The behavior of the beam connection is set as rigid such that the two joined parts will move together during vibration. This behavior is equivalent to the behavior of a fully tightened bolt under dynamic excitation [3, 16, 21].

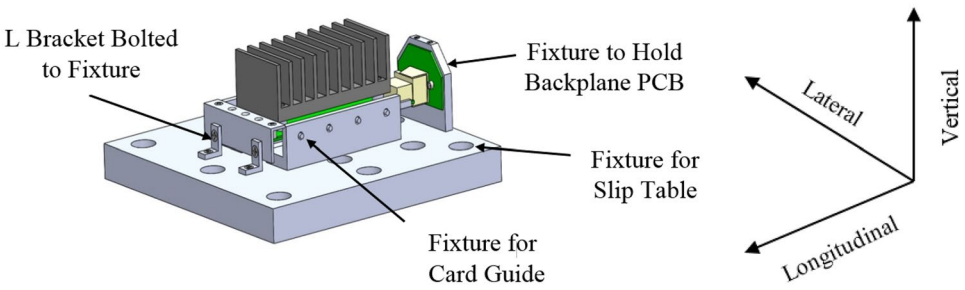

Fig. 12 Single card-level PCB assembly with fixture for simulating base excitation

The connection between the PCB and card guide is modeled as a spring connection to account for the edge guides [13, 14, 16]. The stiffness value of the spring typically depends on the materials used in the spring clips and wedge clamps. This paper assumes the spring clips used in the card guide to be made of beryllium copper (a common material for spring clips used in card guides), with the stiffness value of beryllium copper being used in the analysis. The next step in the FE model is to apply the material properties. The main PCB board is taken as a 6-layered JEDEC PCB board, the PCB board is modeled as an orthotropic model, and the material properties of the JEDEC PCB board as referenced from the literature [10] are listed in Table 3, where the X–Y-Z coordinate system respectively references the length, width, and thickness of the PCB. The material properties for all other components are listed in Table 4.

Once the material properties and the contact conditions are applied to the model shown in Fig. 12, second-order tetra-dominant meshing is generated. A body sizing mesh is used to ensure that the element quality is greater than 0.7. Figure 13 shows the complete mesh model of the PCB card assembly, including the fixture. Fixtures are used in the FE model to provide the boundary conditions for the PCB assembly. The fixed boundary conditions are applied to the holes shown in the slip table fixture, as those holes are used to connect the slip table in a practical scenario. The backplane fixture and the card guide fixtures are connected to the slip table fixture using a beam connection with rigid behavior. The complete mesh model is then simulated in ANSYS using the procedure developed in Sect. 2. The first step in applying this procedure is to perform the modal analysis and connect the modal analysis results to the harmonic analysis. Table 5 shows the modal frequencies of the PC card assembly shown in Fig. 13. As most of the electronic components in real-life applications will see frequencies as high as 1,000 Hz [14], modal frequencies are requested up to 1,000 Hz. Table 5 shows the list of the dominant natural frequencies of the assembly. The first natural frequency is the longitudinal vibration of the PCB board. Since the PCB board is clamped by a face plate along one edge and has spring supports across its length, the unconstrained DOF is the first natural frequency of the system. The shape of the vibration of the PCB board along with the heatsink at first mode natural frequency is shown in Fig. 14. Similarly, the second and third modes respectively represent the vibrations of a PCB along the longitudinal and vertical directions of the PCB.

4.2 Harmonic Vibration Excitation

This section presents the results of the harmonic vibration excitation by applying the procedure developed in Sect. 2.

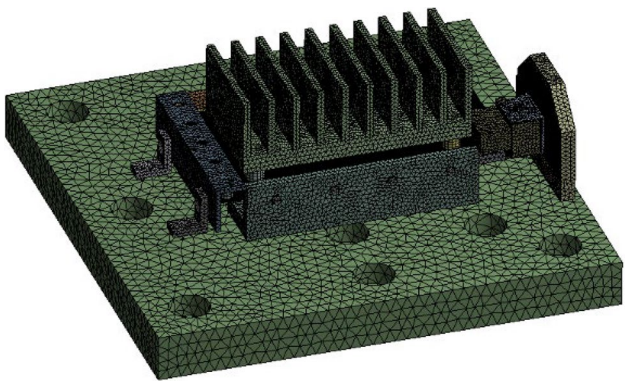

Fig. 13 Complete mesh model of the assembly including the fixtures

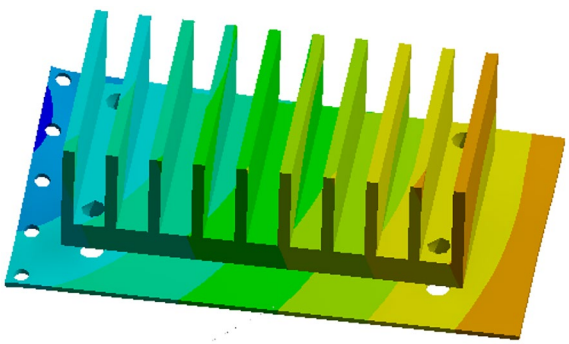

Fig. 14 Vibration of the PCB board and heatsink at the first natural frequency

Table 3 Material Properties for FR4 PCB

Young's Modulus of Elasticity	E_x (pa)	2.3E+10
	E_y (pa)	1.9E+10
	E_z (pa)	0.4E+10
Shear Modulus	G_{xy} (pa)	1.97E+10
	G_{xz} (pa)	1.97E+10
	G_{yz} (pa)	1.97E+10
Poisson's Ratio	υ_{xy}	0.1
	υ_{xz}	0.4
	υ_{yz}	0.38
Mass Density	ρ(Kg/m^3)	1900

The harmonic excitation is carried out in ANSYS using Eq. (9). This is possible by connecting the modal analysis results in the form of mode shapes, modal frequencies, and effective mass to the ANSYS harmonic analysis tool. During the harmonic analysis, the excitation frequency is varied over the frequency range of 5–1000 Hz while keeping the amplitude of base excitation at 1g, where g represents the acceleration due to gravity. The maximum amplitudes of steady-state response from the card connector and backplane connector at each excitation frequency along the excitation direction are recorded and plotted as a function of the excitation frequency. Figure 15 shows the response of the PCB card connector and the backplane connector along the longitudinal direction (card insertion direction). As shown in Fig. 15, the card connector response is around the second and fourth modes of the vibration, and the backplane connector motion is along the third mode of vibration. This result shows the backplane connector response to be solely from the backplane PCB vibration and the card connector response to be from the resonance vibration of the main PCB vibration in the card insertion direction. The relative motion between the card connector and the backplane connector is calculated by taking the absolute difference of the motion as described in Sect. 2. Figure 16 shows the relative motion between the card connector and backplane connector in the card insertion direction (longitudinal). As shown in Fig. 16, the relative motion is maximum around the resonance frequency. An interesting thing to note from Fig. 16 is that the relative motion can be minimized by designing the card connector and the backplane connector to vibrate at the same resonance frequency. The maximum amplitude of relative motion as seen in Fig. 16 is 16.3 microns. Similar results have been reported in the existing literature through experimentation [4, 5, 18]. Figures 17 and 18 represent the relative motion between the card connector and the backplane connector in the lateral and vertical directions. The magnitude of relative motion along the lateral and vertical directions is less compared to the longitudinal direction. This is due to the main PCB board and the backplane PCB board connector having a sliding contact motion along the longitudinal direction, whereas no constraints are applied along the vertical or longitudinal directions.

Table 5 List of Natural Frequencies

Natural Frequencies in (Hz)	160.00
	195.11
	232.12
	398.71

4.3 Random Vibration Excitation

This section presents the results from the random vibration analysis performed on the backplane connection using the procedure developed in Sect. 2. Random vibration signals

Table 4 Material Properties for Various Components

COMPONENT	MATERIAL	DENSITY (Kg/m^3)	YOUNG'S MODULUS (MPa)
PCB	FR4	1900	Table 2
Backplane (Motherboard)	FR4	1900	Table 2
Male Connector Housing	Liquid Crystal Polymer	1400	1.72E+3
Female Connector Housing	Liquid Crystal Polymer	1400	1.72E+3
Heatsink	6061-T6	2720	68E+3
Standoff	6061-T6	2720	68E+3
L-Bracket	6061-T6	2720	68E+3
Card Guide housing	6061-T6	2720	68E+3
Card Guide Spring	Beryllium Copper	8250	125E+3
Fixtures (all)	6061-T6	2720	68E+3

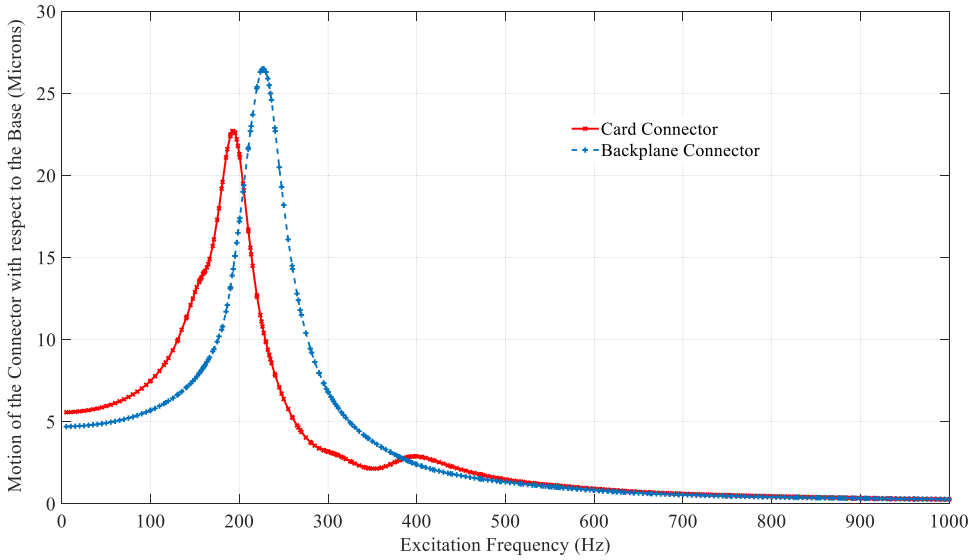

Fig. 15 Amplitude of vibration of the card connector and the backplane connector

are usually presented in the condensed form known as PSD. Section 2 of this paper presents the procedure for developing the pseudo-random time series based on the signal's PSD. In this section, the PSD of the signal is decomposed into pseudo-random time series, and the corresponding pseudo-random time series is implemented in the ANSYS simulation to obtain the relative motion of the mating connectors. The reference PSD signal taken for the analysis is from references [1, 9], "Military Standard for Electronic Component Testing", (MIL), and the "American Association of Railroad Standard", (AAR). A composite PSD profile is generated based on references [1, 9] using the peak hold technique. Figure 19 shows the composite PSD profile based on the MIL and AAR standards. The pseudo-random time series of this composite PSD profile is shown in Fig. 20 and was developed through the procedure mentioned in Sect. 2. To make a correlation between the original PSD and the pseudo-random time series, the PSD is regenerated from the pseudo-random time series. Figure 21 shows the comparison of the original PSD to the regenerated PSD. Based on Fig. 21, all the frequency components of the regenerated PSD and the original PSD are clearly well-correlated. The pseudo-random time series is then used in the ANSYS to simulate the relative motion due to longitudinal, lateral, and vertical excitations. To perform the transient analysis, the modal data are connected to the transient analysis tool as described in Sect. 2, and the transient responses are collected from the card connector and the backplane connector for the longitudinal, lateral, and vertical

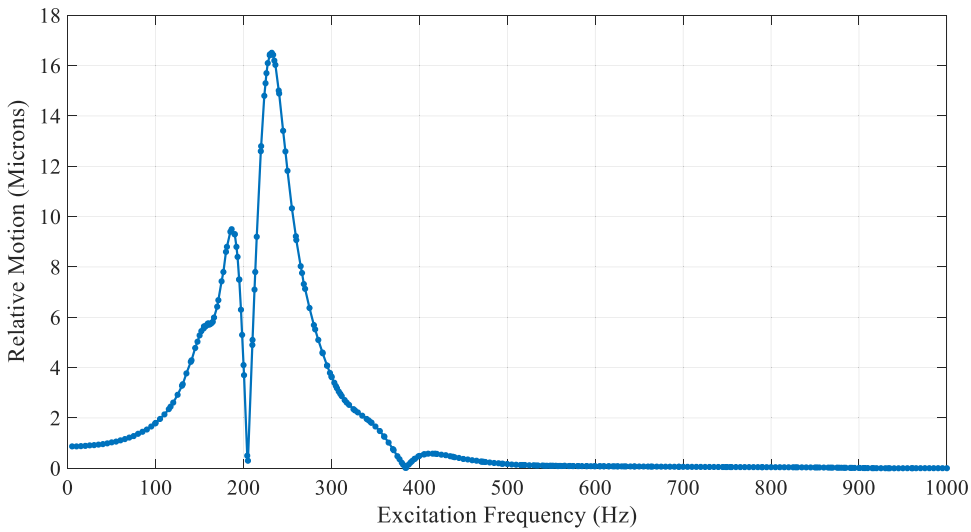

Fig. 16 Relative motion between the card connector and the backplane connector

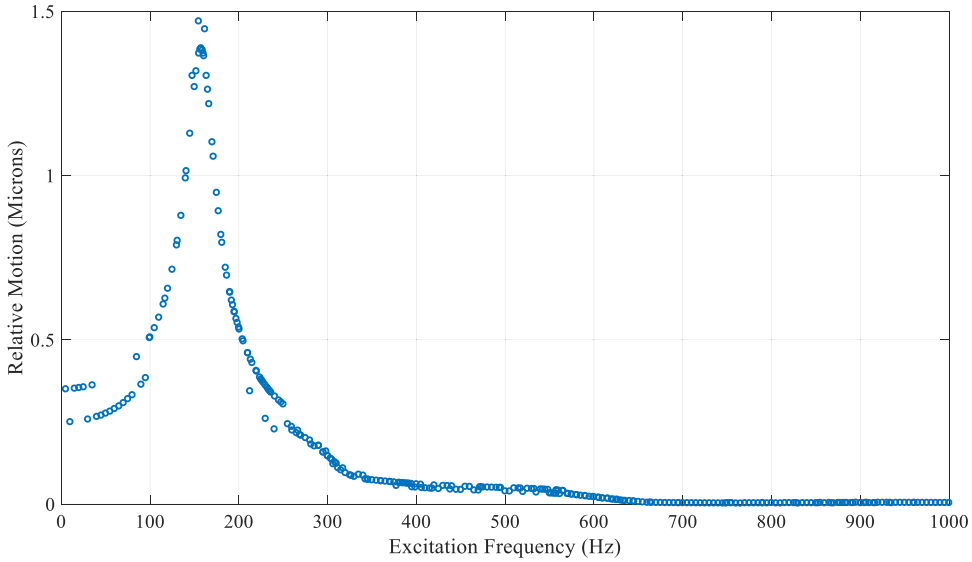

Fig. 17 Relative motion between the card connector and the backplane connector (lateral direction excitation)

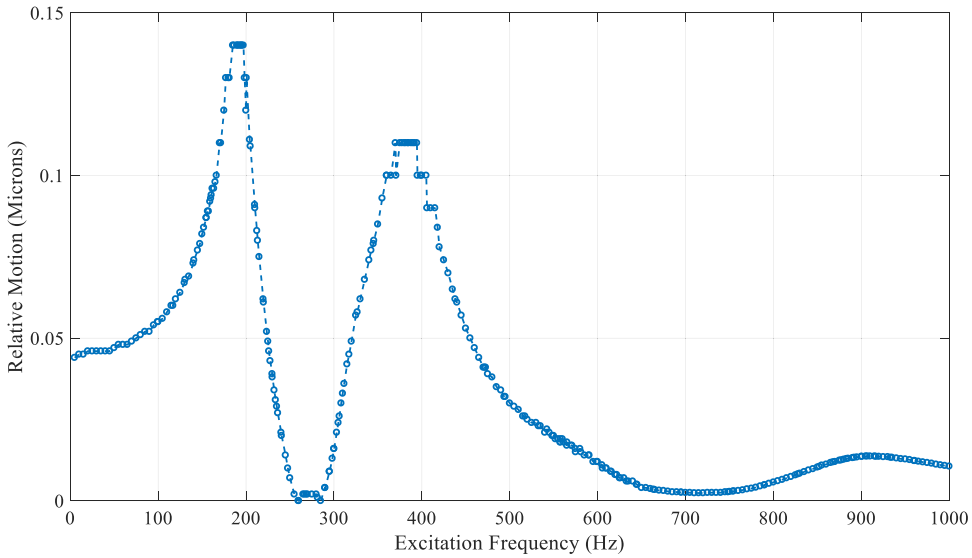

Fig. 18 Relative motion between the card connector and the backplane connector (vertical direction excitation)

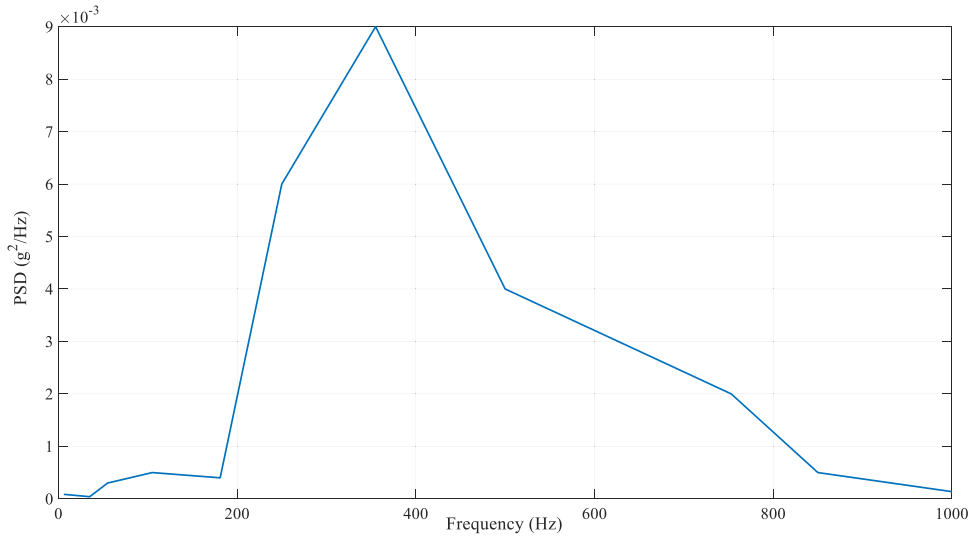

Fig. 19 A composite PSD profile for random vibration excitation ($G_{rms} = 1.65$)

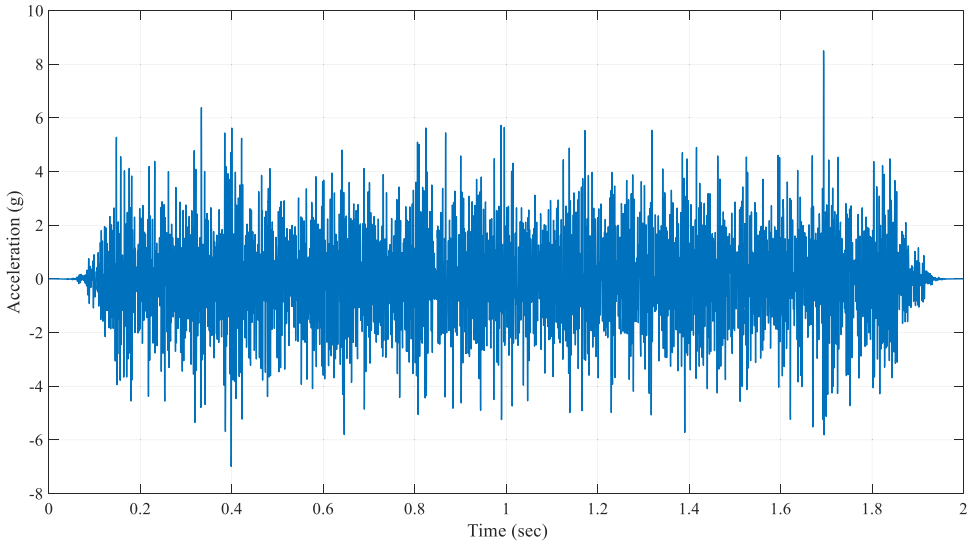

Fig. 20 Pseudo-random time series generated from the PSD ($G_{rms} = 1.645$)

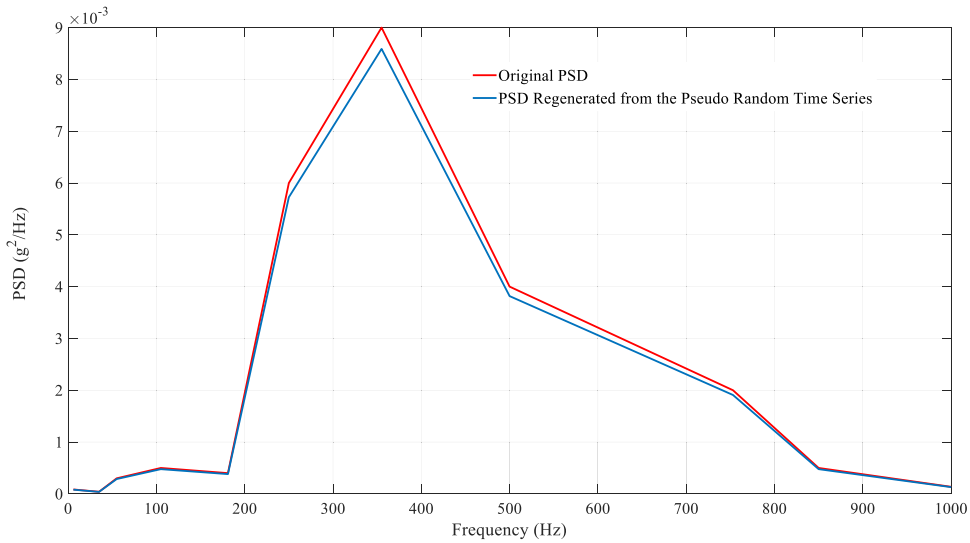

Fig. 21 Comparison of the original and regenerated PSDs

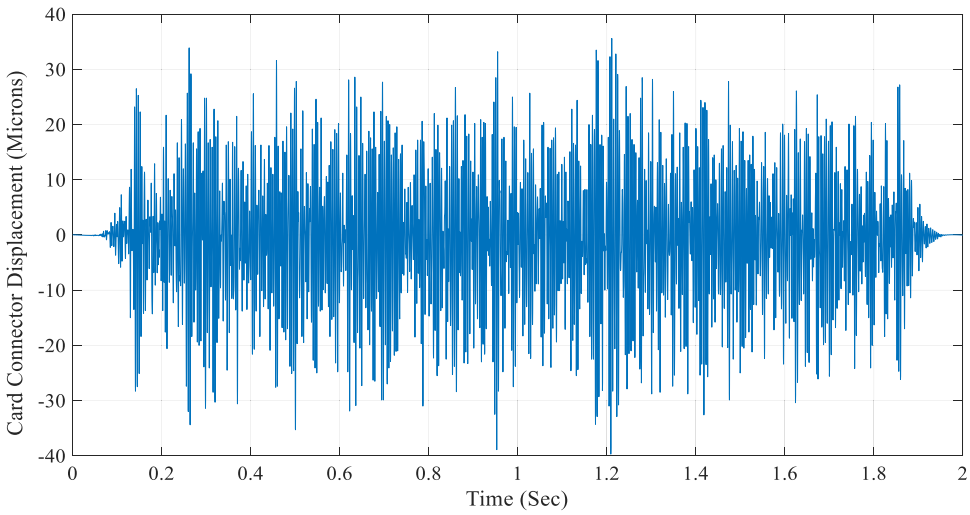

Fig. 22 PCB card connector response along the longitudinal direction

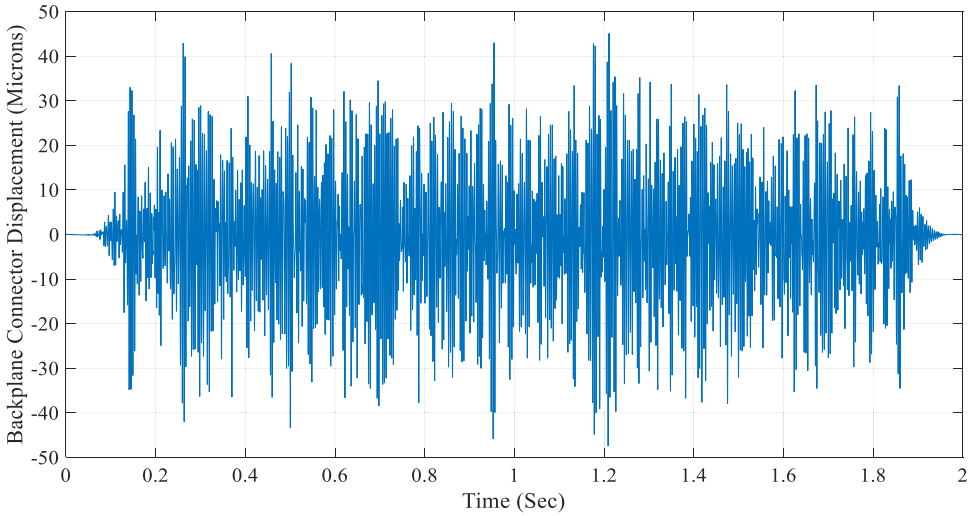

Fig. 23 Backplane connector response along the longitudinal direction

directions. Figure 22 shows the PCB card connector motion along the longitudinal excitation, and Fig. 23 shows the backplane connector motion along the longitudinal direction. The relative motion between the card connector and the backplane connectors is calculated using Eq. (13) and is shown in Fig. 24, with the maximum instantaneous relative motion in the longitudinal excitation being 27.5 microns. As the assembly has resonance frequencies between 150–400 Hz and the excitation signal is maximum around these frequencies, the relative motion is expected to be maximum around these frequencies. To find out the total cumulative movement, Eq. (14) is applied to the data shown in Fig. 24. Table 6 shows the results of the cumulative movement and the maximum amplitude of relative motion along the longitudinal, lateral, and vertical excitation directions. The maximum cumulative relative movement is in the longitudinal direction due to the sliding contact motion between the card connector and the backplane connector in that direction.

4.4 Significance of the Numerical Experimentation Results

The results obtained from the experimentation with the numerical FE-based model show the main source of relative motion within the mating connector to be the coupled dynamics between the PCBs and the mounting brackets. The relative motion will be maximum around the resonant frequency, so the stepped-sine test (harmonic input) is the best approach for computing the maximum relative motion. The pseudo-random time series-based approach will be able to quantify the cumulative relative movement of the mating connector, which is directly related to the degradation of the pin material within the mating connector. The approach and the results presented here are very helpful for studying design of experiments (DOE) regarding pin fretting, for reducing pin fretting through design modification, for reducing pin fretting through the development of active and passive vibration control systems,

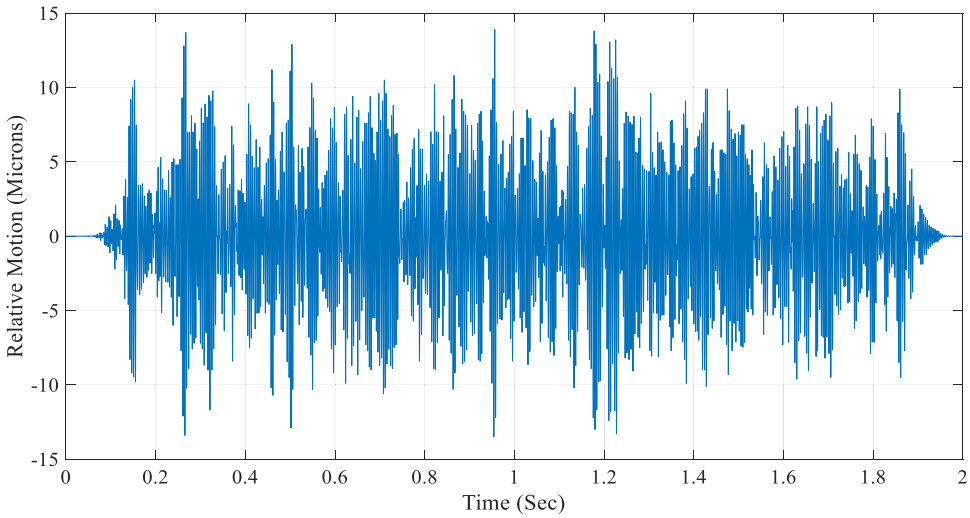

Fig. 24 Relative motion between the card connector and the backplane connector along the longitudinal direction

Table 6 Relative Motion due to Random Vibration Excitation

Excitation Direction	Maximum Amplitude of Relative Motion (Microns)	Cumulative Relative Movement in 2 Sec (Microns)	Cumulative Relative Movement per Sec (Microns)
Longitudinal (Card Insertion Direction)	27.4	9.9277E + 3	4.96385E + 3
Lateral	0.5	237.45	118.725
Vertical	0.358 + 0.12	232.1439	116.071

and for developing material degradation models regarding pin fretting.

5 Conclusion

This paper presents the theoretical methodology for the quantification of relative motion within a mating connector as a measure of pin fretting in PCB connectors. The methodology is based on the dynamics of PCBs, PCBAs, and mounting brackets. Two types of signals (i.e., harmonic and random vibration signals) have been taken into consideration for the analysis. In the harmonic signal analysis, a frequency domain computation approach is presented where the excitation frequency is varied around the natural frequency of the system and the maximum amplitude of response at each excitation frequency is computed. The relative motion within the mating connector is computed by calculating the response difference between the male connector and the female connector at each excitation. The results of the harmonic analysis show the maximum relative motion within the mating connector to occur at the resonant frequency. In the random vibration analysis, the time domain-based approach is presented for computing the relative motion within the mating connector. A pseudo-random time series is generated based on the PSD of the signal, and the generated pseudo-random time series is utilized to excite the system. The mathematical model for computing the cumulative relative movement of the mating connector has also been presented. Two numerical examples are provided to illustrate the overall approach. The first example analyzes a 2 DOF model subjected to base excitation using the harmonic signal and a random white noise time series. The second case develops a numerical model based on finite elements. The numerical model with a backplane connection system is utilized to compute the relative motion between the PCB card connector and the backplane connector, with the results showing a significant amount of relative motion to occur and the total cumulative movement to happen in the direction of the card insertion. The significance of the total cumulative movement is that the pin material degradation in the mating connector can be represented by a simple time series model. Because electronic connectors are subjected to random vibration excitation during in-service conditions, the methodology presented here serves numerous benefits such as: (i) evaluations of vibration thresholds for different connectors used in PCBs, (ii) design of different types of connector systems for vibration environments, (iii) evaluation of the role of floating connector designs with respect to pin fretting, (iv) development of active/passive vibration suppression techniques for reducing pin fretting, and (v) development of a PCB card-clamping mechanism to reduce pin fretting. Future research will focus on the following topics:

(i) Experimental evaluation of backplane connection systems using the developed methodology.
(ii) Improving the theoretical modeling technique using the local–global modeling approach to validate the FE model using experimental data and construct a local model consisting of male and female pins. The displacement boundary condition will be applied to the local model at the pin terminals, and the displacement boundary conditions will be obtained from the global model. The improved method will help in predicting the difference in relative motion between the housing and contact pins.
(iii) Due to the impossibility of measuring relative motion at pins, the maximum amplitude of relative motion will be evaluated using the destructive failure analysis technique. The length of the scar will help in finding maximum peak-to-peak relative motion.
(iv) The material degradation due to pin fretting will be evaluated by measuring the pin coating thickness using cross-sectioning, and the degradation rate will be calculated using the excitation time. In this way, the obtained degradation rate will be compared with the cumulative relative movement developed in this paper.

Data Availability All the data, codes, and simulation files will be provided upon request.

Declarations

Conflicts of Interest All authors declare that they have no conflicts of interest.

References

1. Cackovic DL, Bollock RL (1994) Proposed alternative test procedure for AAR specification M-965–91 with the vibration test

unit. Proceedings of IEEE/ASME Joint Railroad Conference. IEEE
2. Chen C (2009) A study of the prediction of vibration-induced fretting corrosion in electrical contacts. Auburn University
3. Coria I, Martín I, Bouzid A-H, Heras I, Abasolo M (2018) Efficient assembly of bolted joints under external loads using numerical FEM. Int J Mech Sci 142:575–582
4. Flowers GT, Xie F, Bozack MJ, Malucci RD (2004) Vibration thresholds for fretting corrosion in electrical connectors. IEEE Trans Compon Packag Technol 27(1):65–71
5. Flowers GT, Xie F, Bozack M, Horvath R, Rickett BI, Malucci RD (2005) The influence of contact interface characteristics on vibration-induced fretting degradation. Proceedings of the Fifty-First IEEE Holm Conference on Electrical Contacts. pp 82-88
6. Horn J, KourimskyF, BaderschneiderK, Lutsch H (1995) Avoiding fretting corrosion by design. AMP J Technol 4:4–7
7. Hsu S-W, Liao K-C (2012) Wear analysis and verification of metallic terminals for electronic connectors. Eng Fail Anal 25:71–80
8. Huang B, Li X, Zeng Z, Chen N (2016) Mechanical behavior and fatigue life estimation on fretting wear for micro-rectangular electrical connector. Microelectron Reliab 66:106–112
9. Jang J, Park J-W (2020) Simplified vibration PSD synthesis method for MIL-STD-810. Appl Sci 10(2):458
10. Kalyani UH, Wylie M (2020) Modal finite element analysis of PCBs and the role of material anisotropy. Vib Proced 32:75–80
11. Liao K-C, Chang C-C (2009) Applications of damage models to durability investigations for electronic connectors. Mater Des 30(1):194–199
12. Luo Y, Zhang Z, Wu X, Su J (2020) Identification and Sensing of Wear Debris Caused by Fretting Wear of Electrical Connectors. IEICE Trans Electron E103.C(5):246–253
13. Singh P, Viswanadham P (1997) Failure modes and mechanisms in electronic packages. Springer Science & Business Media
14. Steinberg DS (2000) Vibration analysis for electronic equipment, Third Edition, John Wiley & Sons
15. Swingler J, McBride JW (2002) Fretting corrosion and the reliability of multicontact connector terminals. IEEE Trans Compon Packag Technol 25(4):670–676
16. Vandevoordt KP, Feng M (2009) Dynamic Behavior of Electronic Module Spring Clips, Retention Bar, and Backplane Connector: Modeling and Testing. ASME Int Mech Eng Congress Expo 43789:217–223
17. Wu B-H, Lee C-Y, Chiang Y-C, Cao S, Cao X, Zhang G, Zhou S, Wang B (2018) Study on the contact performance of electronic EON connectors under axial vibration. IEEE Trans Compon Packag Manuf Technol 8(12):2090–2097
18. Xie F (2007) A study of vibration-induced fretting corrosion for electrical connectors. Auburn University (Diss)
19. Xing Y, Xu W (2017) Signal Analysis of Fretting Damages on Electrical Connector Systems, Master's Thesis, Blekinge Institute of Technology, Karlskrona
20. Yang H, Tong Y, Flowers G, Cheng Z (2016) Capacitance build-up in electrical connectors due to vibration induce fretting corrosion. In: Proc. IEEE 62nd Holm Conference on Electrical Contacts (Holm), pp 152-158
21. Yang J, Tan CP, He Z, Ching ZY, Tan CC (2017) An effective system-level vibration prediction analysis approach for data storage system chassis. Microsyst Technol 23(9):3097–3105
22. Yu W, Zeng Z, Peng B, Yan S, Hua Y, Jiang H, Li X, Fan T (2018) Multi-Objective Optimum Design of High-Speed Backplane Connector Using Particle Swarm Optimization. IEEE Access 6:35182–35193. https://doi.org/10.1109/ACCESS.2018.2847732

Sushil Doranga is an Assistant Professor at the Lamar University, Beaumont, Texas since September 2019. Prior to joining Lamar, Dr. Doranga worked at General Electric (GE) Canada in the transport intelligence division as a senior engineer. While at GE, Dr. Doranga was instrumental in developing the pin fretting solution for the electronic connectors. Dr. Doranga received his Ph.D. degree in mechanical engineering from the University of Manitoba, Winnipeg, Canada in 2015. His current research interests include structural dynamics, electronic packaging vibration modeling, linear and nonlinear vibration and structural health monitoring. Dr. Doranga has several papers published in the area of mechanical vibrations.

Jenny Zhou is a professor in the Department of mechanical Engineering at Lamar University, Beaumont, Texas. Dr. Zhou received her Ph.D. degree in mechanical Engineering from University of Maryland, Baltimore County. Her research interests include dynamic responses and vibrations of microelectronic systems, Plant Biomechanics, multi-scale and multi-physics modeling and research in engineering education. She has published more than 50 papers in electronics packaging.

Ram Poudel is an assistant professor in the Department of Sustainable Technology & the Built Environment, Appalachian State University, Boone, NC. He received his PhD from University of Massachusetts Amherst in 2017. His research interest include integration of mechatronics to wind energy, Renewable energy storage and integration and energy access and development.